JOURNAL OF AGRICULTURAL AND FOOD CHEMISTRY
ARTICLE

J. Agric. Food Chem. 2010, 58, 12993–12998 12993
DOI:10.1021/jf103723k

Irreversible Competitive Inhibitory Kinetics of Cardol Triene on Mushroom Tyrosinase

Jiang-Xing Zhuang,[†,§] Yong-Hua Hu,[†,§] Mei-Hua Yang,[†] Feng-Jiao Liu,[†] Ling Qiu,[†] Xing-Wang Zhou,*[,‡] and Qing-Xi Chen*[,†]

[†]Key Laboratory of the Ministry of Education for Coastal and Wetland Ecosystems, School of Life Sciences, Key Laboratory for Chemical Biology of Fujian Province, Xiamen University, Xiamen 361005, China, and [‡]Department of Biochemistry and Pharmacology, Zhongshan School of Medicine, Sun Yat-sen University, Key Laboratory of Tropical Disease Control, Ministry of Education, Guangzhou 510080, China. [§]The authors contributed equally to this work.

Cardol triene was first purified from cashew (*Anacardium occidentale* L.) nut shell liquid and identified by gas chromatography coupled to mass spectroscopy and nuclear magnetic resonance. The effects of this compound on the activity of mushroom tyrosinase were studied. The results of the kinetic study showed that cardol triene was a potent irreversible competitive inhibitor and the inactivation was of the complexing type. Two molecules of cardol triene could bind to one molecule of tyrosinase and lead to the complete loss of its catalytic activity. The microscopic rate constants were determined for the reaction of cardol triene with the enzyme. The anti-tyrosinase kinetic research of this study provides a comprehensive understanding of inhibitory mechanisms of resorcinolic lipids and is beneficial for the future design of novel tyrosinase inhibitors.

KEYWORDS: Tyrosinase; cardol triene; inhibitory kinetics; competitive inhibition

INTRODUCTION

Tyrosinase (EC 1.14.18.1), also known as polyphenol oxidase (PPO), is a copper-containing multifunction oxidase widely distributed in microorganisms, animals, and plants. This oxidase catalyzes two distinct reactions of melanin synthesis, the hydroxylation of a monophenol (monophenolase activity) and the conversion of an *o*-diphenol to the corresponding *o*-quinone (diphenolase activity), and is the key factor involved in the formation of melanin pigments (*1*). Certain fruits and vegetables usually suffer from browning during handling, processing, and storage after harvest. Enzymatic browning is a major factor that contributes to the loss of quality in foods and beverages (*2*). Browning usually impairs the sensory properties of products because of the associated changes in color, flavor, and softening, which results in a shorter shelf life and decreases the market value (*3*). Therefore, tyrosinase inhibitors have been established as important constituents of depigmentation agents (*4*) and have potential uses as food preservatives (*5*).

Tyrosinase inhibitors should have broad applications, so much effort has been spent searching for feasible and effective tyrosinase inhibitors. Although a large number of naturally occurring tyrosinase inhibitors have already been reported (*6*), their individual activity is not potent enough to be put into practical use. In addition, the safety regulations for food additives limit their applications in vivo, so we must rely on laboratory synthesis or extraction from plants (*7*) to resolve the problems. In our previous paper, flavonoids (*8*), hexylresorcinol (*9*), dodecylresorcinol (*9*), 3,5-dihydroxyphenyl decanoate (DPD) (*10*), and alkylbenzaldehydes (*11*) were shown to inhibit the enzymatic oxidation of DOPA and the inhibitory kinetic study was performed in detail.

Recently, we purified a cardol triene from cashew (*Anacardium occidentale* L.) nut shell and found it is a potent irreversible competitive inhibitor of tyrosinase. The aim of this paper is, therefore, to conduct a kinetic study of the inhibition of the enzyme.

Cardol triene {$C_{15:3}$, 5-[8(*Z*),11(*Z*),14-pentadectrienyl]resorcinol} is known to be abundantly distributed in Gingkoaceae and Anacardiaceae. Some of them had been reported to possess various biological effects, such as antioxidation effects (*12*), antimicrobial effects (*13*), antitumor effects (*14*), and anti-AchE activity (*15*). The anti-tyrosinase kinetic research will provide a comprehensive understanding of the inhibition mechanism of resorcinolic lipids and is beneficial for the future design of novel tyrosinase inhibitors.

MATERIALS AND METHODS

Chemicals. Dimethyl sulfoxide (DMSO), mushroom tyrosinase, and L-DOPA were purchased from Sigma Chemical Co. (St. Louis, MO).

Separation and Purification of Cardol Triene from Cashew Nut Shell Liquid. The separation method used was similar to that previously described (*16*). In brief, CNSL (cashew nut shell liquid, 100 g) was dissolved in methanol (200 mL), and ammonium hydroxide (25%, 200 mL) was added and the mixture stirred for 15 min. This solution was then extracted with hexane (4 × 200 mL). The organic layer was washed with 5% HCl (100 mL) followed by distilled water (100 mL). Activated charcoal (10 g) was added to the organic layer and the mixture stirred for 10 min and filtered. The filtrate was dried over anhydrous sodium sulfate and concentrated, yielding pure cardanol (65 g). The methanolic ammonia solution was extracted with an ethyl acetate/hexane mixture (4:1) (2 × 200 mL). The resulting organic layer was washed with 5% HCl (100 mL) followed by distilled water (100 mL), dried over anhydrous

*To whom correspondence should be addressed. E-mail: chenqx@xmu.edu.cn (Q.-X.C.) or zhouxw2@mail.sysu.edu.cn (X.-W.Z.).

Published on Web 12/01/2010

sodium sulfate, and concentrated to yield crude cardols (18 g). Cardol triene was further purified by preparative high-performance liquid chromatography (P-HPLC).

P-HPLC. HPLC analysis was conducted on a modular HPLC instrument comprising two 510 reciprocating pumps, an Agilent 1100 Series variable-wavelength detector, and a Rheodyne injector (20 μL loop), all from Waters Corp. A Hypersil ODS 25 μm (4.6 mm × 150 mm) column was used. The mobile phase consisted of acetonitrile, water, and acetic acid (80:20:1) at a flow rate of 1.80 mL/min. Absorbance was monitored at 280 nm. We conducted each analysis by dissolving 25 mg of sample in 5 mL of the mobile phase.

Gas Chromatography and Mass Spectroscopy (GC−MS). GC−MS analysis was conducted using a Varian GC 3800 instrument with a Varian 1200 Quadrupole MS/MS mass spectroscopy instrument, on an Ultra 2 column. The sample (1 mg) was dissolved in 10 mL of dichloromethane, and 1 μL of this solution was injected into the GC−MS setup. The temperature was increased from 50 to 250 °C at a rate of 10 °C/min and maintained at 250 °C for 40 min.

Nuclear Magnetic Resonance (NMR) Spectroscopy. ^{1}H and ^{13}C NMR spectral data were recorded on a Fourier transform Bruker AV 600 spectrometer; the compound was dissolved in 0.5 mL of DMSO-d_6 with 0.03% TMS as the internal reference standard.

Enzyme Assay. The following conditions were used for this experiment. First, mushroom tyrosinase differs from other sources to some degree (*17*), but this fungal source was used because of its ready availability. Second, the mode of inhibition is known to depend on the structure of both the substrate and inhibitor, so L-DOPA was used as the substrate, unless otherwise specified. Therefore, the activity studied is with respect to the *o*-diphenolase inhibitory activity of mushroom tyrosinase. Third, tyrosinase is known to catalyze a reaction between two substrates, a phenolic compound (L-DOPA) and oxygen, but the assay was conducted in air-saturated aqueous solutions. Therefore, the Michaelis constant (K_m) and maximum velocity (V_m) determined under these conditions were only apparent, and the effect of oxygen concentration on these parameters is unknown.

Enzyme activity was determined at 30 °C by following the increase in absorbance at 475 nm (ε = 3700 M^{-1} cm^{-1}) accompanying the oxidation of the substrate (L-DOPA). One unit of enzymatic activity was defined as the amount of enzyme increasing absorbance by 0.001 at 475 nm under this condition. The progress-of-substrate-reaction theory previously described (*18*) was used to study the inhibitory kinetics. In this method, the mushroom tyrosinase [1.0 mg/mL in 0.1 M phosphate buffer (pH 6.8)] was first diluted 50-fold with water, and then 50 μL of the solution was added to 200 μL of an assay substrate solution with 25 μL of DMSO containing different concentrations of cardol triene. The substrate reaction progress curve was analyzed to obtain the reaction rate constants. The reaction was conducted at a constant temperature of 30 °C. The kinetic and inhibition constants were obtained by the method previously described (*19*−*22*).

RESULTS AND DISCUSSION

Purification and Structure Identification of Cardol Triene. CNSL contained an abundance of alkyl phenols such as anacardic acids, cardols, and cardanols and therefore was chosen for the separation of cardol triene. In this study, cardol triene was separated and purified from CNSL as described above. The purity was confirmed by element analysis. Anal. Calcd for cardol triene: C, 80.21; H, 9.62. Found: C, 81.09; H, 10.43. The GC−MS and NMR results were consistent with those previously described (*23*). The GC−MS and NMR analyses were conducted to confirm its structure (**Table 1**). The structure of cardol triene is shown in **Figure 1**.

Effect of Cardol Triene Concentration on Inactivation of Mushroom Tyrosinase. The effects of cardol triene on the oxidation of L-DOPA catalyzed by mushroom tyrosinase were first studied. The activity of mushroom tyrosinase was inhibited in a cardol triene concentration-dependent manner as shown in **Figure 2a**. As the concentrations of cardol triene increased, the remaining enzyme activity was rapidly decreased, and when the cardol triene concentration reached 55 μM, the enzyme activity was completely suppressed. The inhibitor concentration leading to 50% activity lost (IC_{50}) was estimated to be 22.5 μM. If the enzyme was preincubated with cardol triene at different concentrations for 1 h, the inactivation of the enzyme was more obvious and the remaining activity decreased sharply. The IC_{50} was estimated to be 8.0 μM, and at ~26 μM cardol triene, the enzyme was completely inactivated. This observation indicates that the inactivation is an irreversible reaction.

Mechanism of Inhibition of Cardol Triene on Mushroom Tyrosinase. The mechanism of inhibition of the enzyme by cardol triene during the oxidation of L-DOPA was first studied. The relationship between enzyme activity and its concentration in the

Table 1. ^{1}H NMR Spectral Data of Isolated Cardol Triene[a]

atom	δ	signal	J (Hz)
H2	6.05	1H, s	
H4,6	6.03	2H, s	
H1′	2.36	2H, t	7.8
H2′	1.49	2H, m	6.3
H3′,4′,5′,6′	1.30	8H, m	6.3
H7′	2.01	2H, m	4.8, 5.4
H8′,9′	5.34	2H, m	5.4, 10.8
H10′	2.75	2H, t	6
H11′,12′	5.34	2H, m	5.4, 10.8
H13′	2.79	2H, t	6
H14′	5.78	1H, dd	11.2, 16.8
H15′a	4.95	1H, dd	1.2, 11.2
H15′b	5.02	1H, dd	1.2, 16.8

[a] In DMSO-d_6, at 600 MHz, with δ relative to TMS.

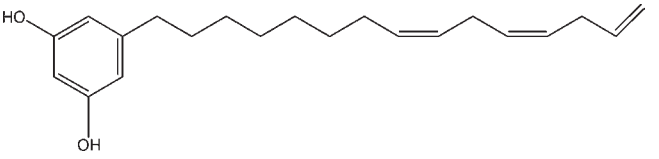

Figure 1. Structure of cardol triene.

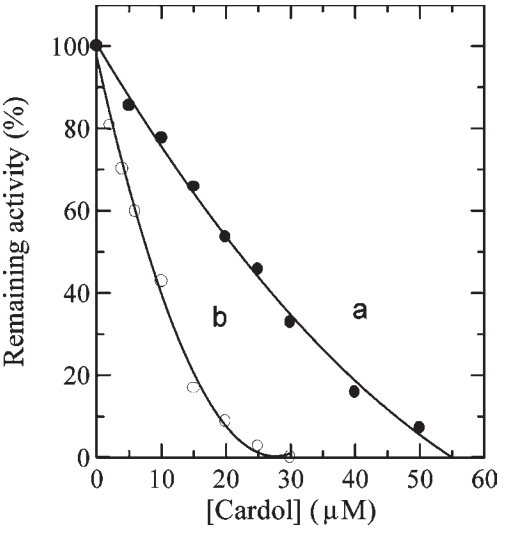

Figure 2. Inactivation of mushroom tyrosinase by cardol triene from CNSL. (**a**) Tyrosinase (20 μg) in a 3 mL reaction system containing 0.05 M sodium phosphate buffer (pH 6.8), 0.5 mM L-DOPA, and different concentrations of cardol triene. The data were recorded after reaction for 1 min. (**b**) Mixture of the enzyme (20 μg) and different concentrations of cardol triene for preincubation for 1 h and then an assay of the remaining activity.

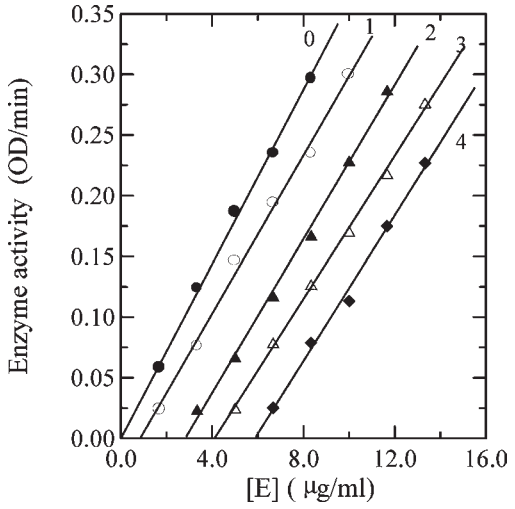

Figure 3. Effect of concentrations of cardol triene on the activity of mushroom tyrosinase for the catalysis of DOPA at 30 °C. Assay conditions: 3 mL reaction system containing 0.05 M sodium phosphate buffer (pH 6.8), 0.5 mM L-DOPA, and different concentrations of cardol triene. Concentrations of cardol triene for curves 0−4 were 0, 10, 20, 30, and 40 μM, respectively.

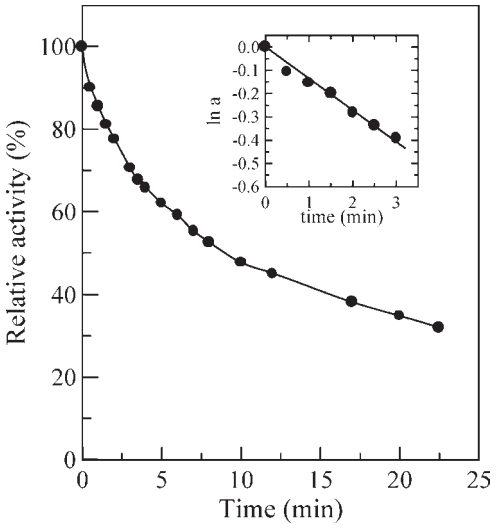

Figure 4. Course of inhibition of mushroom tyrosinase by cardol triene from CNSL. Mixture of the enzyme (20 μg) and cardol triene (15 μM) in 2.7 mL of 0.05 M phosphate buffer (pH 6.8) at 30 °C. At different time intervals as indicated, 0.3 mL of 5.0 mM L-DOPA was added for the determination of the activity at 30 °C with a Spectra MAX plus microplate spectrophotometer. The inset shows a semilogarithmic plot of the results.

presence of different concentrations of cardol triene was determined. The plots of the remaining enzyme activity versus the concentrations of enzyme at different concentrations of cardol triene gave a family of straight lines with different slopes and different abscissa intercepts (**Figure 3**). Increasing the inhibitor concentration resulted in the decrease in the slopes of the lines, but the rate of decrease became slower. When the cardol triene concentration was more than 30 μM, the lines turned parallel to each other. The results indicate that the inactivation of cardol triene on the enzyme was irreversible. The enzyme molecules are first combined with inactivator (cardol triene) fast and reversibly, and then irreversible inactivation occurs. The increasing abscissa intercept indicated that the amount of efficient enzyme decreased by the inactivation.

Kinetics of the Oxidation of L-DOPA Catalyzed by Mushroom Tyrosinase. The kinetic behavior of mushroom tyrosinase in the oxidation of L-DOPA has been studied. Under the conditions employed here, the oxidation reaction of L-DOPA with mushroom tyrosinase follows Michaelis−Menten kinetics. The kinetic parameters for mushroom tyrosinase obtained from a Lineweaver−Burk plot are as follows: K_m = 0.665 mM, and V_{max} = 1481 μM/min. At different concentrations of cardol triene, the double-reciprocal plots yield a family of straight lines with a common intercept on the $1/v$ axis but with different slopes. The results show that the inactivation of the enzyme by cardol triene was a competitive reaction.

Kinetics of Inactivation of Mushroom Tyrosinase by Cardol Triene. The inactivation of mushroom tyrosinase by cardol triene was first studied by the conventional method. The enzyme (20 μg) was first incubated with different concentrations of cardol triene in 2.7 mL of 55 mM phosphate buffer (pH 6.8) at 30 °C. At different time intervals as indicated, 0.3 mL of 5.0 mM L-DOPA was added for the assay of activity at 30 °C. It showed the course of inactivation of the enzyme at a cardol triene concentration of 15 μM. A semilogarithmic plot of the relative activity versus reaction time (t) gives a straight line (see the inset of **Figure 4**), indicating that the inactivation course is a first-order reaction. From the slope of the straight line, the inactivation rate constant and its mushroom tyrosinase activity at other cardol triene concentrations were obtained. The concentrations of cardol triene were 5, 10, 15, 20, and 25 μM with inactivation rate constants of 0.238, 0.738, 2.265, 4.490, and 5.277 × 10^{-3} s^{-1}, respectively. With the increasing cardol triene concentration, the inactivation rate increased.

The inactivation of the enzyme by cardol triene can be expressed as **Schemes 1** and **2**:

Scheme 1

$$E \xrightarrow{k_1} E'$$

Scheme 2

$$E + n\,I \xrightarrow{k_2} EI_n$$

where E and I denote the native enzyme and inactivator (cardol triene), respectively, n denotes the molecule numbers of inactivator (cardol triene) that bound with every molecule of enzyme and leave the enzyme inactivated, and k_1 and k_2 are the first- and second-order rate constants of inactivation of the enzyme, respectively. The relationship between k_1 and k_2 and the inhibitor concentration [I] can be written as follows.

$$k_1 = k_2[I]^n \quad \text{or} \quad \log k_1 = \log k_2 + n \log[I]$$

A plot of log(k_1) versus log[I] gives a straight line, as shown in **Figure 5**, where the slope of the straight line gives the value of n (2.0408). The obtained result shows that every molecule of enzyme must be combined with two molecules of cardol triene and lost its activity.

Kinetics of the Substrate Reaction in the Presence of Different Concentrations of Cardol Triene. The time courses of the oxidation of the substrate, L-DOPA, by mushroom tyrosinase in the presence of different cardol triene concentrations are shown in **Figure 6a**. The results in **Figure 6a** show that, at each concentration of cardol triene, the rate decreased with time until a straight line is approached, the slope of which decreases with an increasing cardol triene concentration. As discussed by Tsou (*17*), the results described above suggest the slow formation of a reversible inactive

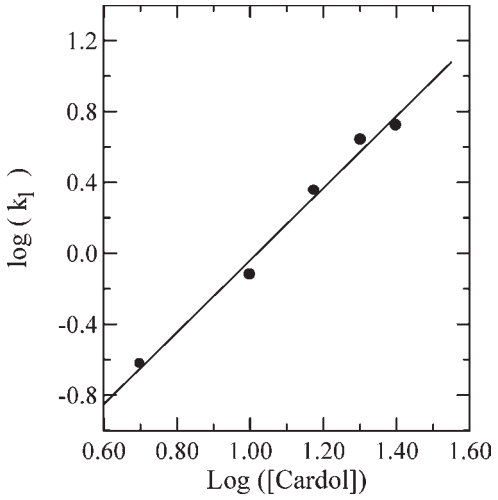

Figure 5. Plot of log(k_1) vs log[cardol triene]. Experimental conditions were as described in the legend of **Figure 4** except for the concentrations of cardol triene. The concentrations of cardol triene were 5, 10, 15, 20, and 25 μM.

enzyme−cardol triene complex. The reaction scheme can be written as **Scheme 3**:

Scheme 3

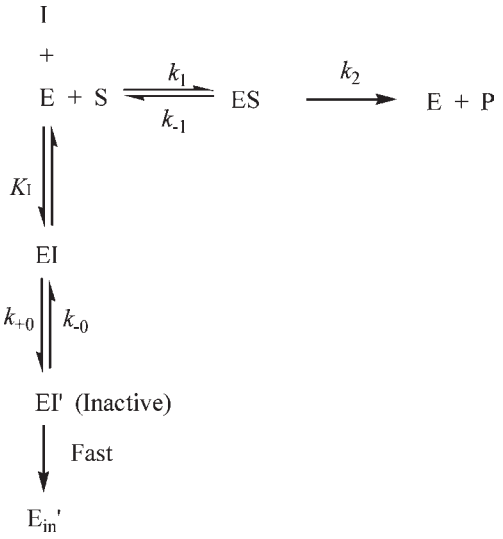

where S, P, I, and E denote the substrate, product, inactivator (cardol triene), and native enzyme, respectively, ES, EI, and EI′ denote the respective complexes, E_{in}' is the dead enzyme, and k_{+0} and k_{-0} are rate constants for forward and reverse inactivation of the enzyme, respectively. The derivation of the kinetic equations has been described previously (*22*). The product formation can be expressed as

$$[P]_t = \frac{v}{A[I]+B}\left\{Bt + \frac{A[I]}{A[I]+B}\left[1 - e^{-(A[I]+B)t}\right]\right\} \quad (1)$$

and

$$A = \frac{\frac{k_{+0}}{K_I}K_m}{K_m\left(1+\frac{[I]}{K_I}\right)+[S]} \quad (2)$$

$$B = k_{-0} \quad (3)$$

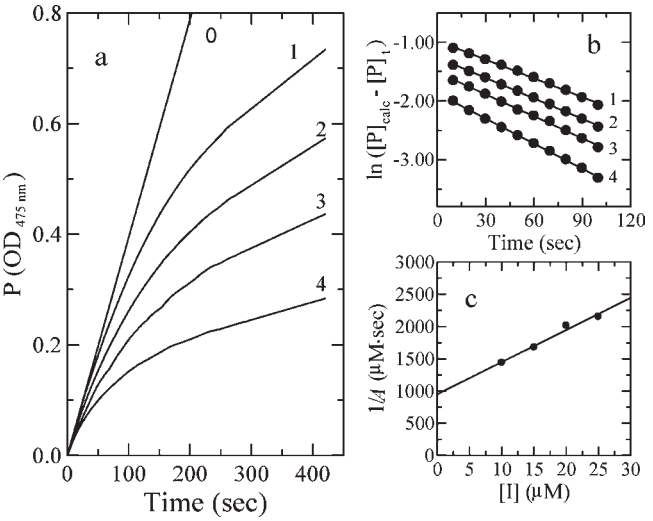

Figure 6. Course of the substrate reaction in the presence of different concentrations of cardol triene. Experimental concentrations were as described in the legend of **Figure 2**. (**a**) Substrate reaction course. The cardol triene concentrations for curves 0−4 were 0, 10, 15, 20, and 25 μM, respectively. (**b**) Semilogarithmic plot of $\ln([P]_{calc} - [P]_t)$ vs time. Data were taken from curves 1−4 in panel **a**. (**c**) Plot of 1/*A* vs cardol triene concentration. The values of the apparent rate constant, *A*, were calculated from data in **Figure 4** through semilogarithmic plots of $\ln([P]_{calc} - [P]_t)$ vs time.

where $[P]_t$ is the concentration of the product formed at time *t*, which is the reaction time, *A* and *B* are the apparent rate constants for the forward and reverse reactions between cardol triene and the enzyme, respectively, [S] and [I] are the concentrations of the substrate and inactivator cardol triene, respectively, *v* is the initial rate of reaction in the presence of inhibitor (cardol triene), K_m is the Michaelis constant, and K_I is the dissociation constant of the enzyme−cardol triene complex.

When *t* is sufficiently large, the curves become straight lines and the product concentration is written as $[P]_{calc}$:

$$[P]_{calc} = \frac{vB}{A[I]+B}t + \frac{vA[I]}{(A[I]+B)^2} \quad (4)$$

Plots of $[P]_{calc}$ versus reaction time (*t*) give a series of straight lines at different concentrations of inhibitor ([I]). The slope is

$$\text{slope} = \frac{vB}{A[I]+B} \quad (5)$$

Combining eqs 1 and 4 yields

$$\ln([P]_{calc} - [P]_t) = \ln\frac{vA[I]}{A[I]+B} - (A[I]+B)t \quad (6)$$

Plots of $\ln([P]_{calc} - [P]_t)$ versus reaction time (*t*) give a series of straight lines at different concentrations of inhibitor ([I]) with slopes of $-(A[I] + B)$ (**Figure 6b**). Because the value of *v* can be determined at special concentrations of substrate and inhibitor, from eq 5, the apparent rate constant *B* can be obtained, and then the apparent rate constant *A* can be obtained from the slope. The results obtained show that the value of *B* is almost the same at different concentrations of cardol triene and directly gives the microscopic rate constant (k_{-0}) for the reverse reaction, and the value was measured to be $(2.617 \pm 0.032) \times 10^{-3}\ s^{-1}$. The value of k_{+0} can be obtained by suitable plots of $1/A$ versus [I] as detailed below. It is well-known that plots of $1/A$ versus [I] can differentiate

complexing types of inactivation according to Tsou's method. **Figure 6** shows the plot of $1/A$ versus [I], indicating that the reaction of cardol triene with mushroom tyrosinase is of the complexing type. The complexing step is fast relative to the subsequent inactivation reaction.

From eq 2, the following equation can be given:

$$\frac{1}{A} = \frac{K_I}{k_{+0}}\left(1+\frac{[S]}{K_m}\right)+\frac{1}{k_{+0}}[I] \quad (7)$$

A plot of $1/A$ versus [I] gives a straight line (**Figure 6c**). As K_m is a known quantity, the microscopic rate constant (k_{+0}) and the dissociation constant (K_I) can be obtained from the slope and intercept of the straight line, respectively. The obtained constants show that K_I was 11.25 μM, k_{+0} was 20.12×10^{-3} s^{-1}, and k_{-0} was 2.617×10^{-3} s^{-1}.

Commercially available cashew (*A. occidentale* L.) nut shell liquid mainly contains phenolic constituents such as anacardic acid, cardanol, and cardol triene, which are resorcinolic lipids with 15-carbon side chains (*24*). Resorcinolic lipids, especially 5-alkylresorcinols, had been reported to have various biological activities because of their natural amphiphilic structures. The antioxidation assays showed that the length of the alkyl chain is crucial to their antioxidation potency (*12*, *25*, *26*). These compounds can also perturb the phospholipid bilayer (*27*) and protect against oxidative damage in *Saccharomyces cerevisiae* (*28*).

In this work, cardol triene was isolated from cashew (*A. occidentale* L.) nut shell liquid and was first found to be a potent irreversible inhibitor to mushroom tyrosinase for the oxidation of L-DOPA. Compared to cardanol and anacardic acid, cardol triene exhibited the highest inhibitory potency (*29*). The structure−activity relationship of tyrosinase inhibitors indicates the presence of a resorcinol moiety could enhance the anti-tyrosinase activity drastically; our research also showed strong agreement with this indication (*30*, *31*). The inhibitory kinetic studies showed that the inhibitory mechanism of cardol triene on tyrosinase diphenolase was of the complexing type. The inactivity kinetics point out that every molecule of mushroom tyrosinase must combine two molecules of cardol triene to lose its activity, and that the irreversible inhibition is of the complexing type. The anti-tyrosinase kinetic research is important because it provides a comprehensive understanding of inhibitory mechanisms of such resorcinolic lipids and is beneficial to the future design of novel tyrosinase inhibitors.

ABBREVIATIONS USED

DMSO, dimethyl sulfoxide; L-DOPA, L-3,4-dihydroxyphenylalanine; CNSL, cashew nut shell liquid; IC_{50}, inhibitor concentration leading to a 50% loss of activity.

LITERATURE CITED

(1) Sanchez-Ferrer, A.; Rodriguez-Lopez, J. N.; Garcia-Canovas, F.; Garcia-Carmona, F. Tyrosinase: A comprehensive review of its mechanism. *Biochim. Biophys. Acta* **1995**, *1247* (1), 1−11.

(2) Friedman, M. Food browning and its prevention: An overview. *J. Agric. Food Chem.* **1996**, *44*, 631−653.

(3) Martinez, M. V.; Whitaker, J. R. The biochemistry and control of enzymatic browning. *Trends Food Sci. Technol.* **1995**, *6*, 195−200.

(4) Likhitwitayawuid, K.; Sritularak, B. A new dimeric stilbene with tyrosinase inhibitory activity from *Artocarpus gomezianus*. *J. Nat. Prod.* **2001**, *64*, 1457−1459.

(5) Scotter, M. J.; Castle, L. Chemical interactions between additives in foodstuffs: A review. *Food Addit. Contam.* **2004**, *21*, 93−124.

(6) Kubo, I.; Kinst-Hori, I. Tyrosinase inhibitors from anise oil. *J. Agric. Food Chem.* **1998**, *46*, 1268−1271.

(7) Kubo, I.; Kinst-Hori, I.; Kubo, Y.; Yamagiwa, Y.; Kamikawa, T.; Haraguchi, H. Molecular design of antibrowning agents. *J. Agric. Food Chem.* **2000**, *48* (4), 1393−1399.

(8) Xie, L. P.; Chen, Q. X.; Huang, H.; Wang, H. Z.; Zhang, R. Q. Inhibitory effects of some flavonoids on the activity of mushroom tyrosinase. *Biochemistry* (*Moscow, Russ. Fed.*) **2003**, *68* (4), 487−491.

(9) Chen, Q. X.; Ke, L. N.; Song, K. K.; Huang, H.; Liu, X. D. Inhibitory effects of hexylresorcinol and dodecylresorcinol on mushroom (*Agaricus bisporus*) tyrosinase. *Protein J.* **2004**, *23* (2), 135−141.

(10) Qiu, L.; Chen, Q. X.; Wang, Q.; Huang, H.; Song, K. K. Irreversibly inhibitory kinetics of 3,5-dihydroxyphenyl decanoate on mushroom (*Agaricus bisporus*) tyrosinase. *Bioorg. Med. Chem.* **2005**, *13*, 6206−6211.

(11) Chen, Q. X.; Song, K. K.; Wang, Q.; Huang, H. Inhibitory effects of Mushroom Tyrosinase by Some Alkylbenzaldehydes. *J. Enzyme Inhib. Med. Chem.* **2003**, *18* (6), 491−496.

(12) Trevisan, M. T.; Pfundstein, B.; Haubner, R.; Wurtele, G.; Spiegelhalder, B.; Bartsch, H.; Owen, R. W. Characterization of alkyl phenols in cashew (*Anacardium occidentale*) products and assay of their antioxidant capacity. *Food Chem. Toxicol.* **2006**, *44* (2), 188−197.

(13) Kubo, I.; Nihei, K.; Tsujimoto, K. Antibacterial action of anacardic acids against methicillin resistant *Staphylococcus aureus* (MRSA). *J. Agric. Food Chem.* **2003**, *51* (26), 7624−7628.

(14) Chandregowda, V.; Kush, A.; Reddy, G. C. Synthesis of benzamide derivatives of anacardic acid and their cytotoxic activity. *Eur. J. Med. Chem.* **2009**, *44* (6), 2711−2719.

(15) de Paula, A. A.; Martins, J. B.; dos Santos, M. L.; Nascente Lde, C.; Romeiro, L. A.; Areas, T. F.; Vieira, K. S.; Gamboa, N. F.; Castro, N. G.; Gargano, R. New potential AChE inhibitor candidates. *Eur. J. Med. Chem.* **2009**, *44* (9), 3754−3759.

(16) Phani Kumar, P.; Paramashivappa, R.; Vithayathil, P. J.; Subba Rao, P. V.; Srinivasa Rao, A. Process for isolation of cardanol from technical cashew (*Anacardium occidentale* L.) nut shell liquid. *J. Agric. Food Chem.* **2002**, *50* (16), 4705−4708.

(17) Tsou, C. L. Kinetics of substrate reaction during irreversible modification of enzyme activity. *Adv. Enzymol. Relat. Areas Mol. Biol.* **1988**, *61*, 381−436.

(18) Chen, Q. X.; Zhang, Z.; Zhou, X. W.; Zhuang, Z. L. Kinetics of inhibition of β-glucosidase from *Ampullarium crossean* by bromoacetic acid. *Int. J. Biochem. Cell Biol.* **2000**, *32* (7), 717−723.

(19) Zhou, X. W.; Zhuang, Z. L.; Chen, Q. X. Kinetics of inhibition of green crab (*Scylla serrata*) alkaline phosphatase by sodium (2,2′-bipyridine) oxodiperoxovanadate. *J. Protein Chem.* **1999**, *18* (7), 735−740.

(20) Zhang, R. Q.; Chen, Q. X.; Xiao, R.; Xie, L. P.; Zeng, X. G.; Zhou, H. M. Inhibition kinetics of green crab (*Scylla serrata*) alkaline phosphatase by zinc ions: A new type of complexing inhibition. *Biochim. Biophys. Acta* **2001**, *1545* (1−2), 6−12.

(21) Chen, Q. X.; Zheng, W. Z.; Lin, J. Y.; Cai, Z. T.; Zhou, H. M. Kinetics of inhibition of green crab (*Scylla serrata*) alkaline phosphatase by vanadate. *Biochemistry* (*Moscow, Russ. Fed.*) **2000**, *65* (9), 1105−1110.

(22) Chen, Q. X.; Zhang, W.; Wang, H. R.; Zhou, H. M. Kinetics of inactivation of green crab (*Scylla serrata*) alkaline phosphatase during removal of zinc ions by ethylenediaminetetraacetic acid disodium. *Int. J. Biol. Macromol.* **1996**, *19* (4), 257−261.

(23) Tyman, J.; Bruce, I. Synthesis and characterization of polyethoxylate surfactants derived from phenolic lipids. *J. Surfactants Deterg.* **2003**, *6*, 291−297.

(24) Grazzini, R.; Hesk, D.; Heininger, E.; Hildenbrandt, G.; Reddy, C. C.; Cox-Foster, D.; Medford, J.; Craig, R.; Mumma, R. O. Inhibition of lipoxygenase and prostaglandin endoperoxide synthase by anacardic acids. *Biochem. Biophys. Res. Commun.* **1991**, *176* (2), 775−780.

(25) Przeworska, E.; Gubernator, J.; Kozubek, A. Formation of liposomes by resorcinolic lipids, single-chain phenolic amphiphiles from *Anacardium occidentale* L. *Biochim. Biophys. Acta* **2001**, *1513* (1), 75−81.

(26) Hladyszowski, J.; Zubik, L.; Kozubek, A. Quantum mechanical and experimental oxidation studies of pentadecylresorcinol, olivetol, orcinol and resorcinol. *Free Radical Res.* **1998**, *28* (4), 359−368.

(27) Stasiuk, M.; Kozubek, A. Membrane perturbing properties of natural phenolic and resorcinolic lipids. *FEBS Lett*. **2008**, *582* (25−26), 3607−3613.
(28) De Lima, S. G.; Feitosa, C. M.; Cito, A. M.; Moita Neto, J. M.; Lopes, J. A.; Leite, A. S.; Brito, M. C.; Dantas, S. M.; Cavalcante, A. A. Effects of immature cashew nut-shell liquid (*Anacardium occidentale*) against oxidative damage in *Saccharomyces cerevisiae* and inhibition of acetylcholinesterase activity. *Genet*. *Mol*. *Res*. **2008**, *7* (3), 806−818.
(29) Kubo, I.; Kinst-Hori, I.; Yokokawa, Y. Tyrosinase inhibitors from *Anacardium occidentale* fruits. *J*. *Nat*. *Prod*. **1994**, *57* (4), 545−551.
(30) Qiu, L.; Chen, Q. X.; Wang, Q.; Huang, H.; Song, K. K. Irreversibly inhibitory kinetics of 3,5-dihydroxyphenyl decanoate on mushroom (*Agaricus bisporus*) tyrosinase. *Bioorg*. *Med*. *Chem*. **2005**, *13* (22), 6206−6211.
(31) Khatib, S.; Nerya, O.; Musa, R.; Tamir, S.; Peter, T.; Vaya, J. Enhanced substituted resorcinol hydrophobicity augments tyrosinase inhibition potency. *J*. *Med*. *Chem*. **2007**, *50* (11), 2676−2681.

Received for review September 26, 2010. Revised manuscript received November 10, 2010. Accepted November 16, 2010. This work was supported by Grant 2010CB530002 from the Ministry of Science and Technology, Grant 31071611 from the Natural Science Foundation of China, and Grant 2010N5013 from the Science and Technology Foundation of Fujian Province.